# The Effect of Nanoclay on the Morphological and Physical Properties of Bitumen/PET/Clay Nanocomposites

**Fakhraddin Alimoradi**
Civil Engineering Department, International Campus of Sharif University of Technology, Kish Island, Iran
Email: f.a.moradi8@gmail.com

**Alireza Khaloo***
Civil Engineering Department, Sharif University of Technology, Tehran, Iran
Email: khaloo@sharif.edu, Tel: +98-912-108-7774

**Morteza Faghihi**
Chemistry and Process Research Department, Niroo Research Institute, Tehran, Iran
Email: mfaghihi@nri.ac.ir

## ABSTRACT

The Strengthening asphalt and bitumen to increase their service life has received much attention in recent years. In this paper, the effect of nanoclay (NC) on the physical, thermal, and rheological properties of bitumen/waste polyethylene terephthalate (PET) composites is investigated. X-ray diffraction (XRD) and transmission electron microscopy (TEM) analyses showed the intercalated and partially exfoliated structure of NC layers. Fourier transform infrared (FTIR) spectra was conducted to evaluate the interactions between NC and bitumen. Morphological observation was performed with a field emission scanning electron microscope (FE-SEM). Thermogravimetric analysis (TGA) is used to measure thermal properties. The frequency sweep tests were done by using a dynamic shear rheometer to obtain storage modulus, phase angle, and rutting factor. Penetration, softening point and ductility tests performed to investigate the physical behavior of the samples. The morphological observations and XRD analyses indicated good dispersion of NC in the PET-modified bitumen matrix. Rheological analyses showed an increase in complex modulus of composites with adding of NC. TGA results showed that the presence of NC improved the thermal resistance of nanocomposites. The results showed that the addition of nanoclay and PET to bitumen binder can improve the performance of road pavements and help preserve the environment.

**Keywords:** Bitumen, Clay, Nanocomposites, Physical Properties, Morphology

## 1. Introduction

Asphalt pavements are usually subjected to loads applied while using by various external factors, including mechanical loads due to vehicle movement and thermal loads because of changes in weather conditions [1,2]. These loads can damage the bitumen and lead to some defects such as rutting, cracking and reducing the service life of asphalt pavements [3,4]. Improving the properties of the asphalt binder, i.e. bitumen is a way to reduce the destructive effects of external agents on pavement's performance [5]. Fibers and polymers are among the additives which can enhance the mechanical and thermal resistance of asphalt mixes [6-8]. Polymers are viscoelastic materials that can extend the service temperature of bitumen in various external conditions. In recent decades, the incorporation of polymers in bitumen has been considered to alter the performance of bituminous binders [9-11]. Various polymers including thermoplastic elastomer are utilized in bitumen mixes such as polyethylene (PE) [12-14], styrene butadiene styrene (SBS) [15-17], ethylene propylene diene monomer (EPDM) [18], polyvinyl chloride (PVC) [19,20] and Polyethylene terephthalate (PET) [21,22]. Therefore, the influence of adding polymer to bitumen is investigated in this research.

PET as a thermoplastic polymer has semi-crystalline structure [23]. PET is widely used in various applications such as packaging of food and liquid materials, automotive parts and electronic tools [24]. The high consumption of PET along with its excellent mechanical strength and good thermal resistance has led to the use of recycled PET in various fields such as asphalt binder. The main part of waste PET is made from recycled drinking bottles which leads to environmental hazards. The reusing of waste PET as an additive in bitumen could be a way for waste PET recycling [25]. Maharaj et al. investigated the effect of both concentration and particle size of waste PET [26]. They reported that the higher particle size of waste PET causes higher complex shear moduli. Ahmad and Ayob used 9 wt. % PET in bitumen grade 80/100 and declared that addition of PET caused improving in bitumen properties [27]. Research sources showed that better mechanical and physical performance (decrease in penetration and ductility) with the incorporation of PET into the bitumen. The suitable properties of PET led to the use of this material in this research to improve the properties of the bituminous matrix. The viscoelastic manner of PET could help the performance of the bituminous matrix and provide the basis for the better performance of road pavements.

Nanoclay (NC) as a natural mineral can be used to reinforce polymer-modified bitumen composites [28]. Many types of clay are in the form of aluminosilicates that have layered structures [29]. One of the most important layered nanoclays is montmorillonite (MMT) which has 1 nm of thickness and a high aspect ratio. The excellent geometry structure and extraordinary thermal and mechanical properties of NC have led to its use in the reinforcement of various polymer-modified bitumen such as bitumen/SBS/clay [30,31], bitumen/PE/clay [32-34], bitumen/rubber/clay [35,36], bitumen/PVC/clay [37] and bitumen/EVA/clay [38]. To the best of our knowledge, the use of NC in bitumen/PET composites has not been widely discussed in the literature. Oldham et al. have recently investigated the effect of MMT on the resistance against moisture damage of asphalt pavement [39]. They reported that both PET and MMT are effective in diverting acids from the interface of bitumen and stones leading to more resistance to moisture of asphalt pavement. The aim of this paper is to investigate the effect of different amounts of NC on the physical, morphological, thermal and rheological properties of bitumen/PET composite. Adding PET to bitumen can help in environmental sustainability and recycling of polymer materials. Also, the presence of nanoclay in bitumen and asphalt will be a new solution in improving the properties and performance of the road surface. The use of nanoclay in bitumen/asphalt composite promises the wide application of this compound in road pavements. In addition, the use of nanoclay in pavement construction can be industrially economical and useful. So in this research, the addition of NC to the bitumen/PET matrix is investigated and the various properties of nanocomposites are studied.

## 2. Materials and Methods

Bitumen 60/70 was supplied from Pasargad Refinery of Tehran. The main characteristics of bitumen are shown in **Table 1**.

Recycled PET was prepared from a local company. The modified NC was purchased from SPIC Co. (Nanoclay-SPIC, Cloisite 15A, density <0.85g/cm3, moisture <2%). For the preparation of the samples, the bitumen was heated at 170°C for 5 min. After that, 5 wt. % of PET was added to the melt and mixed in a high rotational mixer (Pakzist Modern, Iran) for another 5 min. Then the NC (at 0.5, 1, 2 and 4 wt. %) was added to the melt sample and the mixing was continued to 40 min. The formulation of all samples is shown in **Table 2**.

The X-ray diffraction (XRD) analysis of the samples was conducted in both low ($2\theta=0.8$-$10°$) and high ($2\theta=10$-$80°$) angle ranges using XRD diffractometer (Philips PW1730) with a wave-length $\lambda=0.15405$ nm, 40 kV, 30 mA and steps size of 0.05°. The Fourier transform infrared (FTIR) spectra were recorded with an FTIR spectrometer (Thermo Nicolet Avatar 360). The morphology of modified bitumen was obtained using a field emission scanning electron microscope (FE-SEM) (TESCAN MIRA3) from gold-coated samples. For more accurate morphological observations, transmission electron microscopy (TEM) was used using Philips EM 208S at 100 kV. The thermal stability of the samples was studied by thermo gravimetric analysis (TGA) using METTLER TOLEDO (Switzerland) TGA/DSC1. The samples (10.0 ± 1.0 mg) were heated under nitrogen at a temperature ranging from 25 to 600°C, at a heating rate of 10 °C/min. The rheological characterization of the neat and modified bitumen was carried out using Anton Paar rheometer (MCR 300). The frequency sweep tests were performed by plate-and-plate geometry (25 mm diameter, 1 mm gap) at 60°C within the linear viscoelasticity region. Physical properties including penetration (25°C), softening point and ductility (25°C), were conducted in accordance with ASTM D36, D5 and D113, respectively.

## 3. Results and Discussion

The low angle XRD patterns of NC, bitumen (B), bitumen/PET (B-P) and bitumen/PET/NC nanocomposites are shown in **Figure 1**. The diffraction peak of NC is positioned at $2\theta=3.1°$ ($d_{001}$-reclection) which is corresponded to d-spacing 26.4 °A, based on $n\lambda=2d\sin\theta$, the Bragg formula, where n=1 and λ=0.154 nm is the wavelength of the X-ray. It is clear that the d-spacing of NC is shifted to the lower angle for bitumen/PET/NC samples. The initial interlayer spacing of samples B-P-0.5C, B-P-1C, B-P-2C, and B-P-4C are 43.1, 39.2, 36.0 and 29.9 °A, respectively. The peak intensity of B-P-4C is more than other nanocomposites. It shows that intercalated structures are formed at higher content of NC. However, in lower NC, the intensity of d001 peaks is reduced and widened which indicates that an intercalated and partially exfoliated structure is formed [30]. The molten bitumen and PET chains could penetrate easier into the clay interlayer galleries due to high-speed shearing, resulting in a partially exfoliated structure [32,40].

In **Figure 2**, the different morphologies of bitumen/polymer/clay composites are shown. As it is seen, the increase in nanoclay layer space resulted in a larger surface area. Applying shear stress during the mixing process increases the interlayer distance. As a result, the polymer and the molten bitumen penetrate into the interlayer galleries of NC which in turn can enhance the distance between the layers.

The high-angle XRD results of the samples are shown in **Figure 3**. The broad peak near 2θ=18° is attributed to bitumen [40]. The distinct peak around 2θ=21° is observed for NC which is also detected for all nanocomposites. The peak around 2θ=21° is for crystalline phase of PET chains with Miller indices of 110 [41].

The infrared spectrum of clay, base bitumen (B), bitumen/PET (B-P) and bitumen/PET/NC nanocomposites are shown in **Figure 4**. For clay, the distinct peaks at 3430 and 1040 $cm^{-1}$ can be represented primary amine stretching and C-H stretching peaks, respectively [42]. For the bitumen sample, the peaks at 2929 and 2850 $cm^{-1}$ represent the C-H vibration. The other peaks of bitumen at 1450, 1375 and 721 $cm^{-1}$ are assigned C-H bending of CH2, C-H bending of CH3 and C-H bending of aromatic, respectively [40,43,44]. The peak at 3430 $cm^{-1}$ is disappeared for bitumen/PET/NC nanocomposites. It can be attributed to the chemical interaction between NC and bitumen [45]. Moreover, the peak around 1030 $cm^{-1}$ in all nanocomposites may be due to split ones from stretching vibration of Si-O and can be attributed to the changing interlayer spacing of NC that results from the shearing in a mixing [46]. As it is seen in FTIR spectra of bitumen/PET/NC nanocomposites, the intensity of peak at 1030 $cm^{-1}$ is increased with the rise in NC content, which may represent more intercalation of NC layers.

The low and high-resolution SEM images of NC are shown in **Figures 5a** and **5b**, respectively. It can be seen that some agglomerates of NC are formed which may be due to high surface energy. While in the high-resolution image of SEM, delamination of NC lamellas is observed. Moreover, as can be seen in **Figures 5a** and **5b**, in some regions there are large clumps with thousands of nanoclay platelets sticking to each other. It may be attributed to the organo-modification of NC [32]. This delaminated and exfoliated structure can lead to better interaction between bituminous matrix, PET chains, and nano-layers of clay lamellas [32,36].

The SEM images of bitumen (B), B-P, B-P-1C and B-P-4C are shown in **Figure 6**. The bitumen shows homogeneity in its surface (**Figure 6a**) which is reported in the literature [45]. The PET fiber can be observed in B-P sample (**Figure 6b**) which implies good interaction between PET and bitumen matrix [26]. This tangled form of PET are also shown in B-P-1C sample (**Figure 6c**) and indicates the network structure of polymer, bitumen and clay can play a bridging role throughout the matrix [47]. In the B-P-1C & B-P-4C nanocomposites images (**Figure 6c** and **d**, respectively) the white particles may be represented the NC. It can be said that NC showed good interaction with bitumen. Furthermore, the good dispersion of NC is observed that may be indicated that NC has two main roles including compatibilizer between bitumen and PET and the mechanical reinforcement of the nanocomposites [48].

TEM imaging is used for additional microstructure information of nanocomposites. Intercalation and exfoliation of NC layers can be detected by using TEM technique. The TEM images of NC and B-P-4C are shown in **Figure 7a** and **b**, respectively. The dark lines correspond to NC layers. As it can be seen from **Figure 7a**, the dimension of NC appears to range between 1 nm to 150 nm which is reported in the literature [49]. In the B-P-4C (**Figure 7b**), the intercalation and delamination of NC layers can be observed. It shows that bitumen melt could penetrate into the NC galleries and lead to good dispersion of NC throughout the bitumen matrix [50,51].

To determine thermal characteristics such as thermal stability and degradation temperature, the TGA studies can be used. **Figure 8** shows TGA curves and the corresponding derivative thermogravimetric (DTG) curves for clay, bitumen, B-P and bitumen/PET/NC nanocomposites. As it is shown, the thermal stability of clay is very higher than bitumen and B-P samples. The weight loss of clay is lower than 30% in the 600°C and it can be ascribed to the high thermal resistance of clay as an inorganic material. Several changes in the rate of weight loss with respect to temperature changes can be observed for nanoclay (**Figure 8a & b**). The weight loss (around 5 wt.%) below 200°C of clay can be due to the presence of water in clay particles and the weight loss after 250°C can be related to the dehydroxylation of the silicate structure [52]. Also, for temperatures lower than 300 °C, changes in the slope of weight loss can be seen in several points for NC (**Figure 8b**).

The onset temperature of thermal degradation ($T_{onset}$), 50% weight loss temperature ($T_{50\%}$), and maximum decomposition temperature ($T_{max}$) of the samples obtained from TGA curves are shown in **Table 3**. As it is seen in this table, with the addition of NC to bitumen matrix, the thermal degradation temperatures were increased. The highest increase in T50% and Tmax are observed for B-P-4C. It can be because of the barrier function of the exfoliated lamellas of NC, which showed at XRD and TEM findings. The intercalation and exfoliation of NC through the bitumen matrix make a tortuous pathway that act as a thermal obstructing and shielding effects that enhances the thermal stability of nanocomposites [46,53].

As it is seen in **Figure 9**, the diffusion path of oxygen through the composite depends on the orientation and distribution of NC in the bitumen matrix. Further separation of the clay layers creates more tortuous paths against the penetration of oxygen, thereby increasing the thermal resistance of the nanocomposite. The XRD analysis and morphological observations (especially TEM) indicated that NC layers are properly intercalated. This delamination of layers could hinder the oxygen paths through the composite and turn the direct path (**Figure 9a**) into tortuous one (**Figure 9b**). Although, additional tests are needed to accurately diagnose the paths and porosity of the composite.

Frequency sweep tests were conducted on all samples at 60°C to evaluate the rheological behavior under different loading rates. **Figure 10a** and **b** show the complex modulus (G*) and phase angle (δ) of based bitumen and its nanocomposites, respectively. The complex modulus of bitumen is increased with the addition of NC especially in lower frequencies which is reported in the literature [54]. G* represents the stiffness of the samples [29]. The increase in G* with the addition of NC may be caused by intercalation and exfoliation of NC layers in bitumen which is shown in XRD and TEM results [55]. This result suggests that NC can enhance the viscoelastic properties of bitumen. In the exfoliation, NC particles are separated from each other and cause a higher surface area for interaction with the matrix. The bitumen molecules and PET chains could interact with NC surface through the Vander Waals forces. So, more intercalation and exfoliation of NC can lead to better interactions and intramolecular connections between the matrix and nanoclay, resulting in increased mechanical properties, stiffness, and elastic response [56].

As it is shown in **Figure 10b**, the δ of the sample is decreased with addition of NC. A greater δ represents a more viscous behavior and smaller δ value indicates a more elastic one [57]. The decline in δ exhibits the higher elasticity of the sample [40]. This reduction in δ with adding of NC represents an improvement in elastic response and confirms the formation of exfoliation structure [28,29,55].

The rutting factor (G*/sinδ) shows the combined effect of both complex modulus and phase angle. According to Strategic Highway Research Program (SHRP) specifications, the rutting factor is the rheological parameter of bitumen which represents the permanent deformation under repeating loads [28]. The rutting factor values should be greater than 1000 pa at 1.6 Hz for the bitumen matrix at the maximum of design temperature [55]. **Figure 11** represents the rutting factor versus frequency for bitumen and its nanocomposites. It shows that with adding of NC to bitumen, the G*/sinδ values is escalated especially in lower frequencies. It shows that NC is more helpful for the enhancement of rutting resistance [55]. Additionally, according to SHRP, bitumen and its nanocomposites satisfies the performance standard value of the rutting factor.

The effect of clay content on the softening point and penetration is shown in **Figures 12a** and **b**, respectively. As it is seen, the addition of NC to bitumen is caused expansion in softening point. The most increase in softening point is observed in B-P-4C (61 °C) which is shown 22% enhancement in softening point compared to bitumen. The rise in softening point of asphalt binder can indicate the pavement resistance against climate change [49]. So, the addition NC to bitumen can lead to better performance of binder in a warm climate which is due to higher thermal resistance that is shown in TGA results. Penetration values of bitumen is decreased with the addition of PET and NC (**Figure 12b**). The addition of NC to B-P samples caused a little reduction in penetration values. Improvement in penetration values can represent better pavement performance especially in traffic loads [49].

The penetration index (PI) is utilized to evaluate the temperature sensitivity of the binder [45]. Penetration depth and softening point are used to estimate PI value. Equation 1 presents the PI value as follows:

$$\mathrm{PI} = \frac{1952-500LogP_{25}-20T_{soft}}{50LogP_{25}-T_{soft}-120} \qquad (1)$$

Where $P_{25}$ and $T_{soft}$ are the penetration value at 25 °C (in 0.1 mm) and softening point temperature (in °C), respectively. A higher PI value indicates lower thermal sensitivity. The PI for road pavement construction are recommended in a range of -2 to +2 values [45]. The calculated PI of all samples are observed in **Table 4**. With the addition of NC to bitumen binder, the PI values are increased compared to base bitumen (B) and B-P samples. This indicates higher thermal resistivity of binder resulting in better pavement performance in higher ambient temperatures. Higher surface area, good interaction and proper dispersion of NC throughout the bitumen binder could enhance the thermal resistance of bituminous pavements.

**Table 4** shows ductility values of bitumen/PET/NC nanocomposites. As it is seen, with rise in NC values, the ductility of samples is increased. The most ductility values is observed at B-P-4C which is shown around 38% enhancement in ductility compared to B-P sample. Ductility can be the indication of elongation or extension ability of bitumen binder. The presence of NC promotes the elongation function of bitumen binder under tension mode. It may be because of proper dispersion and interaction between clay and bitumen/PET (refer to TEM and XRD findings) which caused better mechanical properties. Moreover, the better ductility may result in higher crack resistance which is caused by clay lamella through the bituminous matrix [46].

## 4. Conclusions

The bitumen/PET/NC nanocomposites were successfully prepared by melt mixing. XRD results indicated that intercalated and partially exfoliated structures were formed in the nanocomposites. FTIR spectra revealed an interaction between NC and bitumen. Morphological observations (SEM and TEM) approved the proper NC dispersion throughout the bituminous binder. TGA results showed an enhancement in thermal resistance of bitumen/PET composites by adding NC. The frequency sweep tests indicated that the complex modulus is increased and the phase angle is decreased with the addition of NC to the bitumen/PET. Furthermore, with adding of NC to bitumen, the $G^*/\sin\delta$ values were increased especially in lower frequencies. With the incorporation of NC to bitumen, the increase in softening point and PI and decrease in penetration values was observed which shows better mechanical behavior of nanocomposites compared to bitumen sample. The summary of the results showed that the bitumen/PET/NC composite acts as an effective option in improving road surface performance and can be widely used on pavements in the future.

## ACKNOWLEDGMENTS

The authors acknowledge financial supports provided by the Iran Nanotechnology Initiative Council. The authors also thank Technical and Soil Mechanics Lab. Company of Tehran.

## AUTHOR CONTRIBUTIONS

The authors confirm contribution to the paper as follows: study conception and design: A. Khaloo, M. Faghihi; data collection: F. Alimoradi; analysis and interpretation of results: F. Alimoradi, A. Khaloo, M. Faghihi; draft manuscript preparation: F. Alimoradi, A. Khaloo, M. Faghihi. Allauthors reviewed the results and approved the final version of the manuscript.

## REFERENCES

1 Nguyen, H. Q. H. and Maekawa, K., "Multi-Scale Simulation for Fatigue Life Evaluation of Concrete Pavement subjected to Moving Load under Dry and Wet Conditions", *J. Adv. Concr. Technol.*, **18** (3), pp. 95-115 (2020).

2 Huang, Y., Liu, Z.-h., Liu, J.-y. et al., "Laboratory study on mechanical properties of composite pavement under partial compression-shear load", *Construction and Building Materials*, **356**, pp. 129240 (2022).

3 Shafabakhsh, G., Taghipoor, M., Sadeghnejad, M. et al., "Evaluating the effect of additives on improving asphalt mixtures fatigue behavior", *Constr. Build. Mater.*, **90**, pp. 59-67 (2015).

4 Liu, S., Xu, Y., and Zhou, S., "Evaluation of UV aging behaviors of polyphosphoric acid (PPA) modified asphalt and its asphalt mixture", *Sci. Iran.*, **27** (5), pp. 2247-2257 (2020).

5 Shaban, W. M., Yang, J., Su, H. et al., "Quality improvement techniques for recycled concrete aggregate: a review", *J. Adv. Concr. Technol.*, **17** (4), pp. 151-167 (2019).

6 Modarres, A. and Hamedi, H., "Effect of waste plastic bottles on the stiffness and fatigue properties of modified asphalt mixes", *Mater. Des.*, **61**, pp. 8-15 (2014).

7 Truong, G. T., Son, M.-K., and Choi, K.-K., "Mechanical performance and durability of latex-modified fiber-reinforced concrete", *J. Adv. Concr. Technol.*, **17** (2), pp. 79-92 (2019).

8 Malidarreh, N., Shooshpasha, I., Mirhosseini, S. et al., "Effects of recycled Polyethylene terephthalate fibers on strength behavior of cemented Babolsar sand", *Sci. Iran.*, **27** (3), pp. 1130-1143 (2020).

9 Zhu, J., Birgisson, B., and Kringos, N., "Polymer modification of bitumen: Advances and challenges", *Eur. Polym. J.*, **54**, pp. 18-38 (2014).

10 Khattak, M. J. and Baladi, G. Y., "Fatigue and permanent deformation models for polymer-modified asphalt mixtures", *Transp. Res. Rec.*, **1767** (1), pp. 135-145 (2001).

11 Asgharzadeh, S. M. and Tabatabaee, N., "Rheological master curves for modified asphalt binders", *Sci. Iran.*, **20** (6), pp. 1654-1661 (2013).

12 Attaelmanan, M., Feng, C. P., and Al-Hadidy, A., "Laboratory evaluation of HMA with high density polyethylene as a modifier", *Constr. Build. Mater.*, **25** (5), pp. 2764-2770 (2011).

13 Liang, M., Xin, X., Fan, W. et al., "Comparison of rheological properties and compatibility of asphalt modified with various polyethylene", *Int. J. Pavement Eng.*, **22** (1), pp. 11-20 (2021).

14 Abdel-Raheem, A., Dulaimi, A., Mohamed, A. S. et al., "Investigating the Potential of High-Density Polyethylene and Nano Clay Asphalt-Modified Binders to Enhance the Rutting Resistance of Asphalt Mixture", *Sustainability*, **15** (18), pp. 13992 (2023).

15 Zhang, H., Zhu, C., Tan, B. et al., "Effect of organic layered silicate on microstructures and aging properties of styrene–butadiene–styrene copolymer modified bitumen", *Constr. Build. Mater.*, **68**, pp. 31-38 (2014).

16 Kaya, D., Topal, A., Gupta, J. et al., "Aging effects on the composition and thermal properties of styrene-butadiene-styrene (SBS) modified bitumen", *Constr. Build. Mater.*, **235**, pp. 117450 (2020).

17 Guo, R., "Analysis of influencing factors on rutting resistance of stone matrix asphalt mixtures", *Sci. Iran.*, **27** (3), pp. 1039-1049 (2020).

18 Kumar, A., Choudhary, R., and Kumar, A., "Characterisation of asphalt binder modified with ethylene–propylene–diene–monomer (EPDM) rubber waste from automobile industry", *Road Mater. Pavement Des.*, **22** (9), pp. 2044-2068 (2021).

19 Arabani, M. and Yousefpour Taleghani, M., "Rutting behavior of hot mix asphalt modified by polyvinyl chloride powder", *Pet. Sci. Technol.*, **35** (15), pp. 1621-1626 (2017).

20 Padhan, R. K., Sreeram, A., and Mohanta, C. S., "Chemically recycled polyvinyl chloride as a bitumen modifier: synthesis, characterisation and performance evaluation", *Road Mater. Pavement Des.*, **22** (3), pp. 639-652 (2021).

21 Aldagari, S., Kabir, S. F., and Fini, E. H., "Investigating aging properties of bitumen modified with polyethylene-terephthalate waste plastic", *Resour. Conserv. Recycl.*, **173**, pp. 105687 (2021).

22 Perca Callomamani, L. A., Hashemian, L., and Sha, K., "Laboratory investigation of the performance evaluation of fiber-modified asphalt mixes in cold regions", *Transp. Res. Rec.*, **2674** (7), pp. 323-335 (2020).

23 Moghaddam, T. B., Soltani, M., and Karim, M. R., "Experimental characterization of rutting performance of polyethylene terephthalate modified asphalt mixtures under static and dynamic loads", *Constr. Build. Mater.*, **65**, pp. 487-494 (2014).

24 Zander, N. E., Gillan, M., and Lambeth, R. H., "Recycled polyethylene terephthalate as a new FFF feedstock material", *Addit. Manuf.*, **21**, pp. 174-182 (2018).

25 Taherkhani, H. and Arshadi, M. R., "Investigating the creep properties of PET-modified asphalt concrete", *Civ. Eng. Infrastruct. J.*, **51** (2), pp. 277-292 (2018).

26 Maharaj, C., Maharaj, R., and Maynard, J., "The effect of polyethylene terephthalate particle size and concentration on the properties of asphalt and bitumen as an additive", *Prog. Rubber Plast. Recycl.*, **31** (1), pp. 1-23 (2015).

27 Ahmad, M. and Ayob, M. B., "Improvement of Asphaltic Concrete by Using Waste Polyethylen Terephthalate (PET)", *International Journal of Innovative Research in Science, Engineering and Technology (IJIRSET)*, **4** (8), (2016).

28 Galooyak, S. S., Dabir, B., Nazarbeygi, A. E. et al., "Rheological properties and storage stability of bitumen/SBS/montmorillonite composites", *Constr. Build. Mater.*, **24** (3), pp. 300-307 (2010).

29 Farias, L. G. A., Leitinho, J. L., Amoni, B. d. C. et al., "Effects of nanoclay and nanocomposites on bitumen rheological properties", *Constr. Build. Mater.*, **125**, pp. 873-883 (2016).

30 Golestani, B., Nam, B. H., Nejad, F. M. et al., "Nanoclay application to asphalt concrete: Characterization of polymer and linear nanocomposite-modified asphalt binder and mixture", *Constr. Build. Mater.*, **91**, pp. 32-38 (2015).

31 Babagoli, R., Mohammadi, R., and Ameri, M., "The rheological behavior of bitumen and moisture susceptibility modified with SBS and nanoclay", *Pet. Sci. Technol.*, **35** (11), pp. 1085-1090 (2017).

32 Fang, C., Yu, R., Zhang, Y. et al., "Combined modification of asphalt with polyethylene packaging waste and organophilic montmorillonite", *Polym. Test.*, **31** (2), pp. 276-281 (2012).

33 Mohammadiroudbari, M., Tavakoli, A., Aghjeh, M. K. R. et al., "Effect of nanoclay on the morphology of polyethylene modified bitumen", *Constr. Build. Mater.*, **116**, pp. 245-251 (2016).

34 Babagoli, R., "Laboratory Evaluation of the Effect of Warm Mix Asphalt Additive on the Performance of Bitumen and Asphalt Mixture Containing Polypropylene Waste and Nanoclay", *Journal of Transportation Research*, **20** (3), pp. 419-442 (2023).

35 Yu, J., Ren, Z., Yu, H. et al., "Modification of asphalt rubber with nanoclay towards enhanced storage stability", *Mater.*, **11** (11), pp. 2093 (2018).

36 Ren, Z., Zhu, Y., Wu, Q. et al., "Enhanced storage stability of different polymer modified asphalt binders through nano-montmorillonite modification", *Nanomater.*, **10** (4), pp. 641 (2020).

37 Fang, C., Liu, X., Yu, R. et al., "Preparation and properties of asphalt modified with a composite composed of waste package poly (vinyl chloride) and organic montmorillonite", *J. Mater. sci. Technol.*, **30** (12), pp. 1304-1310 (2014).

38 Siddig, E. A., Feng, C. P., and Ming, L. Y., "Effects of ethylene vinyl acetate and nanoclay additions on high-temperature performance of asphalt binders", *Constr. Build. Mater.*, **169**, pp. 276-282 (2018).

39 Oldham, D., Mallick, R., and Fini, E. H., "Reducing susceptibility to moisture damage in asphalt pavements using polyethylene terephthalate and sodium montmorillonite clay", *Constr. Build. Mater.*, **269**, pp. 121302 (2021).

40 Abdelrahman, M., Katti, D. R., Ghavibazoo, A. et al., "Engineering physical properties of asphalt binders through nanoclay–asphalt interactions", *J. Mater. Civ. Eng.*, **26** (12), pp. 04014099 (2014).

41 Gaonkar, A. A., Murudkar, V. V., and Deshpande, V. D., "Comparison of crystallization kinetics of polyethylene terephthalate (PET) and reorganized PET", *Thermochimica Acta*, **683**, pp. 178472 (2020).

42 Yelkovan, S., Yilmaz, D., and Aksoy, K., "A study of organo-modified clay type on pet-clay based nanocomposite properties", *Usak Uni. J. Mater. Sci.*, **3** (1), pp. 33 (2014).

43 Yao, H., You, Z., Li, L. et al., "Rheological properties and chemical analysis of nanoclay and carbon microfiber modified asphalt with Fourier transform infrared spectroscopy", *Constr. Build. Mater.*, **38**, pp. 327-337 (2013).

44 Ashour, A., Kareem, M., and Al-Baiati, M. N., presented at the IOP Conference Series: Materials Science and Engineering, 2020 (unpublished).

45 Moussa, G. S., Abdel-Raheem, A., and Abdel-Wahed, T., "Effect of Nanoclay Particles on the Performance of High-Density Polyethylene-Modified Asphalt Concrete Mixture", *Polymers*, **13** (3), pp. 434 (2021).

46 Fang, C., Yu, R., Li, Y. et al., "Preparation and characterization of an asphalt-modifying agent with waste packaging polyethylene and organic montmorillonite", *Polym. Test.*, **32** (5), pp. 953-960 (2013).

47 Yu, R., Fang, C., Liu, P. et al., "Storage stability and rheological properties of asphalt modified with waste packaging polyethylene and organic montmorillonite", *Appl. Clay Sci.*, **104**, pp. 1-7 (2015).

48 Kosma, V., Hayrapetyan, S., Diamanti, E. et al., "Bitumen nanocomposites with improved performance", *Constr. Build. Mater.*, **160**, pp. 30-38 (2018).

49 Khodary, F., "Longer fatigue life for asphalt pavement using (SBS@ clay) nanocomposite", *Int. J. Curr. Eng.*, **5** (2), pp. 949-954 (2015).

50 Zamanizadeh, H., Shishesaz, M., Danaee, I. et al., "Investigation of the corrosion protection behavior of natural montmorillonite clay/bitumen nanocomposite coatings", *Prog. Org. Coat.*, **78**, pp. 256-260 (2015).

51 Favakeh, M., Bazgir, S., and Karbasi, M., "Dynamically vulcanized thermoplastic elastomer nanocomposites based on linear low-density polyethylene/styrene-butadiene rubber/nanoclay/bitumen: Morphology and rheological behavior", *Iran. Polym. J.*, **29** (3), pp. 209-217 (2020).

52 Liu, G., Wu, S., Van de Ven, M. et al., "Influence of sodium and organo-montmorillonites on the properties of bitumen", *Appl. Clay Sci.*, **49** (1-2), pp. 69-73 (2010).

53 Bhargava, S., Raghuwanshi, A. K., and Gupta, P., "Nanomaterial Compatibility and Effect on Properties of Base Bitumen Binder and Polymer Modified Bitumen", *Int. J. Innov. Sci. Eng. Technol.*, **3** (6), pp. 276-282 (2016).

54 You, Z., Mills-Beale, J., Foley, J. M. et al., "Nanoclay-modified asphalt materials: Preparation and characterization", *Constr. Build. Mater.*, **25** (2), pp. 1072-1078 (2011).

55 Yu, J., Zeng, X., Wu, S. et al., "Preparation and properties of montmorillonite modified asphalts", *Mater. Sci. Eng. A* . **447** (1-2), pp. 233-238 (2007).

56 Nguyen, Q. T. and Baird, D. G., "An improved technique for exfoliating and dispersing nanoclay particles into polymer matrices using supercritical carbon dioxide", *Polymer*, **48** (23), pp. 6923-6933 (2007).

57 Zare-Shahabadi, A., Shokuhfar, A., and Ebrahimi-Nejad, S., "Preparation and rheological characterization of asphalt binders reinforced with layered silicate nanoparticles", *Constr. Build. Mater.*, **24** (7), pp. 1239-1244 (2010).

## Figure Captions:

**Figure 1. Low angle XRD patterns of clay, bitumen and bitumen/PET/NC nanocomposites.**

**Figure 2. Schematic illustration of micro-composite, intercalated and exfoliated nanocomposites of bitumen/polymer/NC.**

**Figure 3. High angle XRD patterns of clay, bitumen and bitumen/PET/NC nanocomposites.**

**Figure 4. FTIR spectrum of clay, bitumen and bitumen/PET/NC nanocomposites.**

**Figure 5. Low (a) and high (b) resolution SEM images of NC.**

**Figure 6. SEM graphs of (a) B, (b) B-P, c) B-P-1C and d) B-P-4C samples.**

**Figure 7. TEM images of (a) NC and (b) B-P-4C samples.**

**Figure 8 TGA thermograms (a) weight loss (%) and (b) derivative weight loss (%/°C) of the samples.**

**Figure 9. Oxygen diffusion model through a) bitumen/polymer blend and b) bitumen/polymer/clay nanocomposites.**

**Figure 10. a) Complex modulus, G* and b) phase angle, δ of bitumen, B-P and bitumen/PET/NC nanocomposites.**

**Figure 11. Rutting factor (G*/sinδ) of bitumen, B-P and bitumen/PET/NC nanocomposites.**

**Figure12. a) Softening point and b) penetration of bitumen/PET/clay samples.**

## Table Captions:

**TABLE 1 Main characteristics of bitumen 60/70**

**TABLE 2 Formulation of all samples**

**TABLE 3 Decomposition temperatures from TGA curves of bitumen/PET/NC nanocomposites**

**TABLE 4 PI and ductility values of bitumen/PET/NC nanocomposites**

**Figures:**

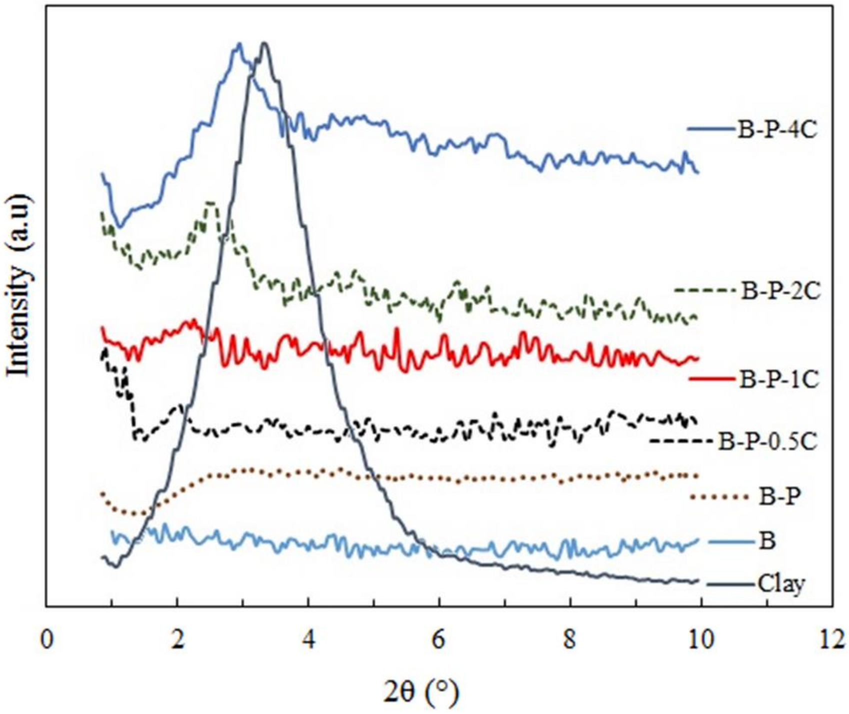

Figure 1

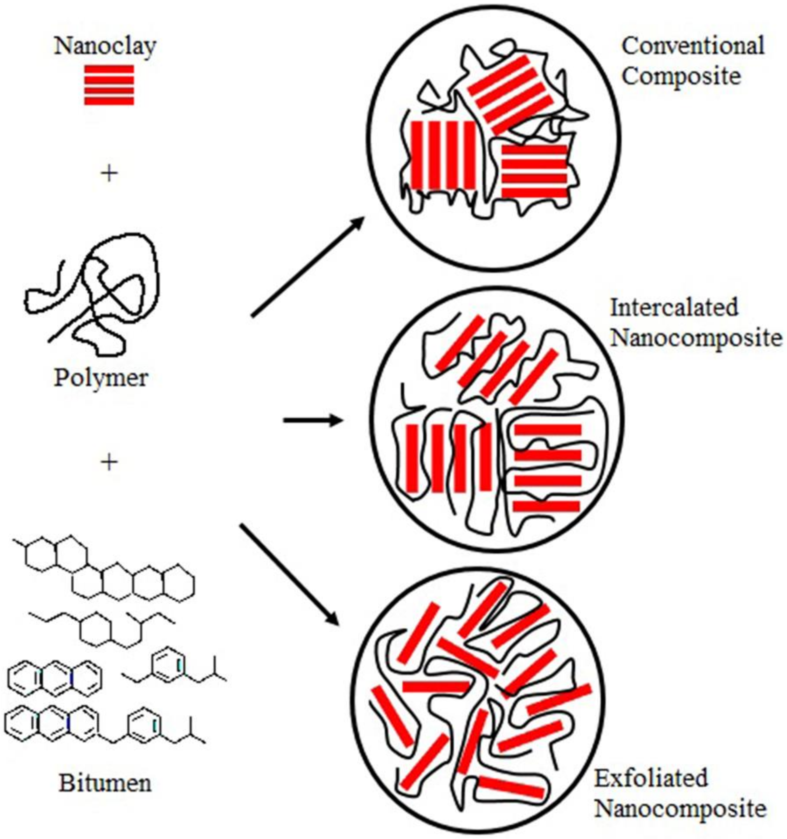
Nanoclay
+
Polymer
+
Bitumen
Conventional Composite
Intercalated Nanocomposite
Exfoliated Nanocomposite

**Figure 2**

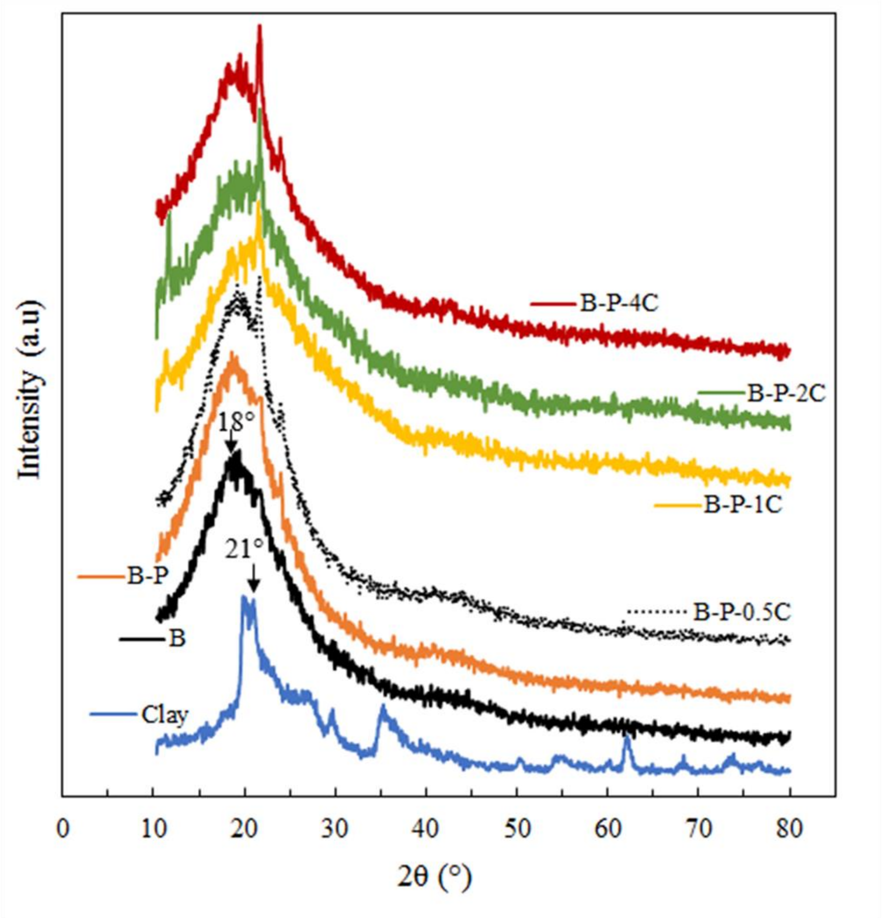
Intensity (a.u)
2θ (°)
0
10
20
30
40
50
60
70
80
B-P-4C
B-P-2C
B-P-1C
B-P-0.5C
B-P
B
Clay
18°
21°

**Figure 3**

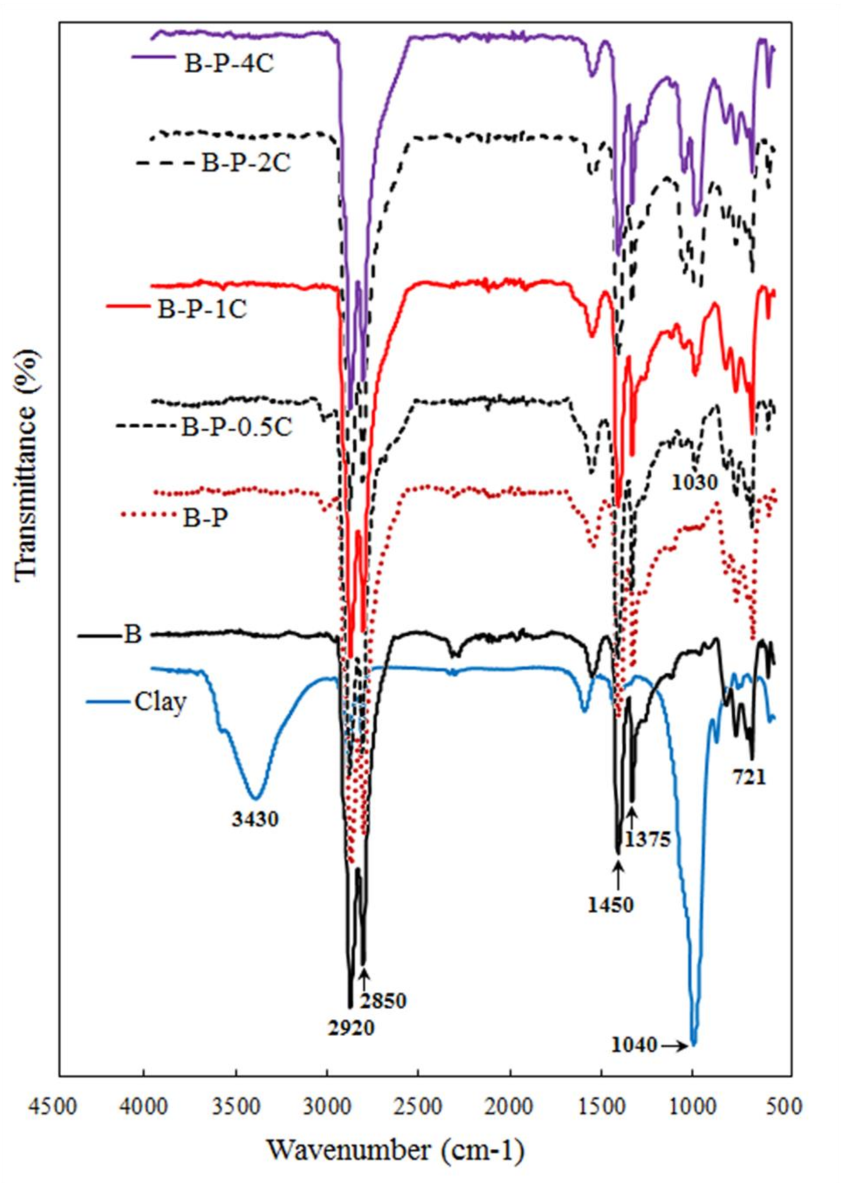
B-P-4C
B-P-2C
B-P-1C
B-P-0.5C
B-P
B
Clay
Transmittance (%)
3430
2920
2850
1450
1375
1040
1030
721
4500
4000
3500
3000
2500
2000
1500
1000
500
Wavenumber (cm-1)

Figure 4

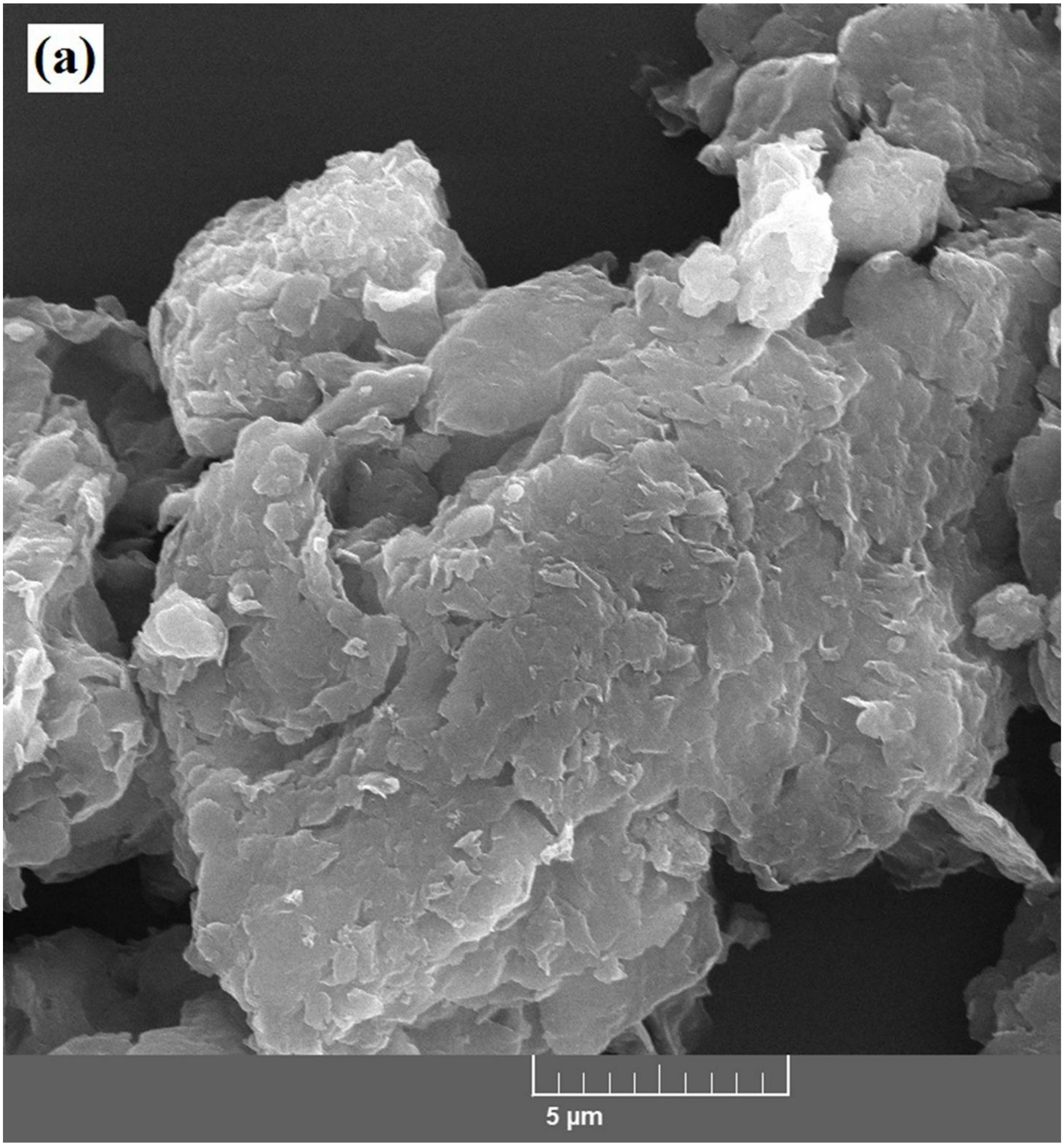

Figure 5 (a)

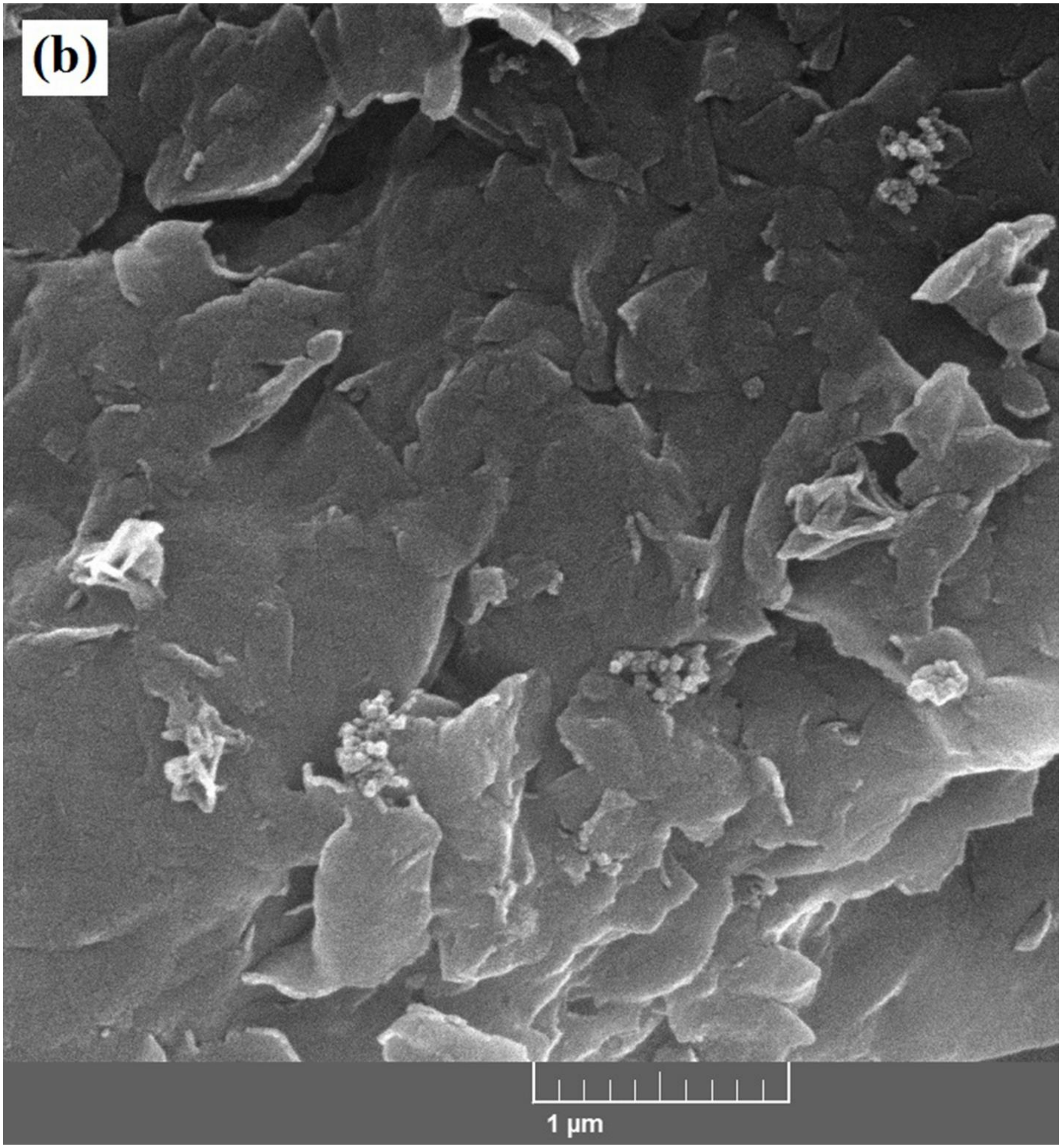

Figure 5 (b)

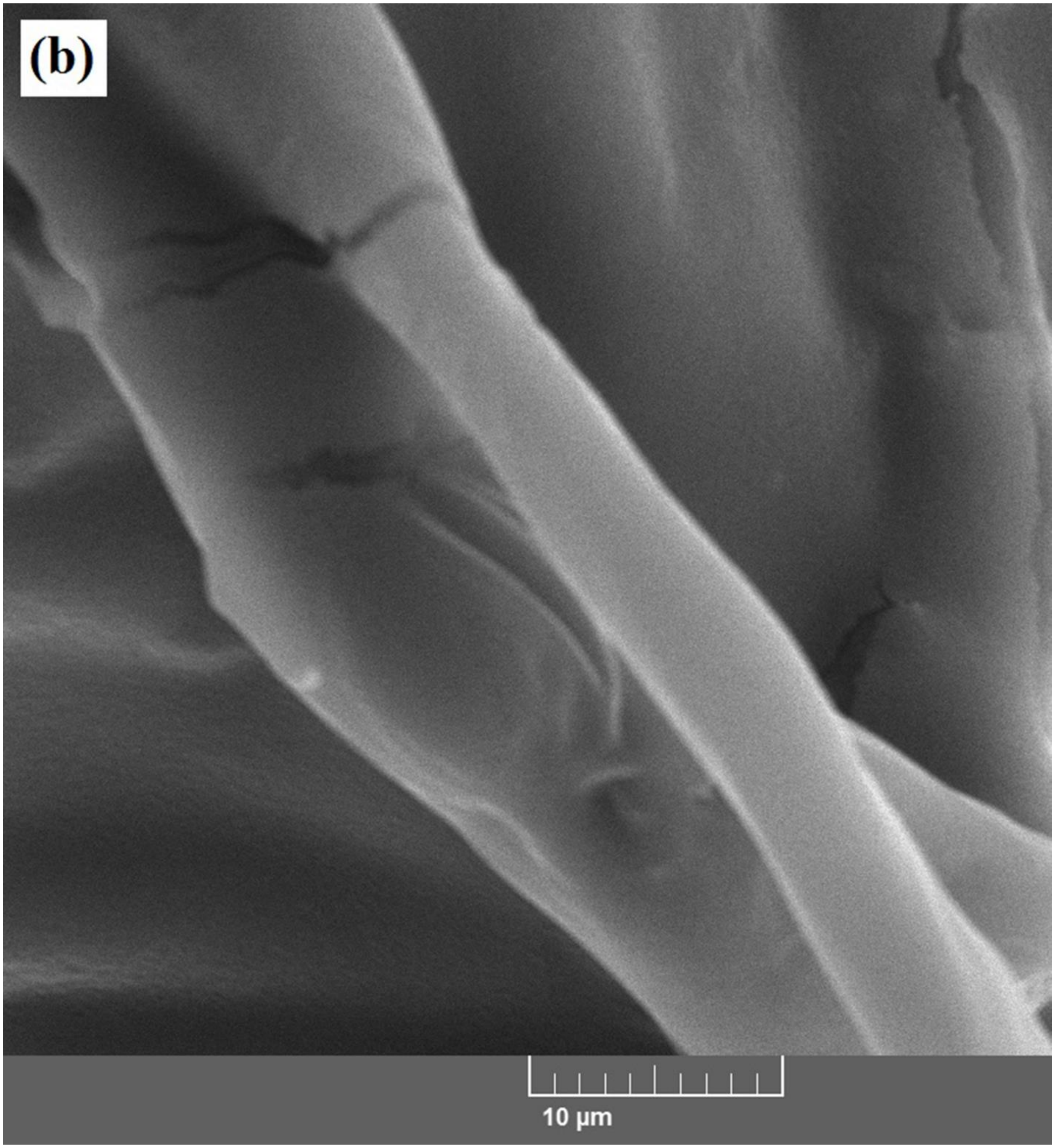
(b)
10 µm

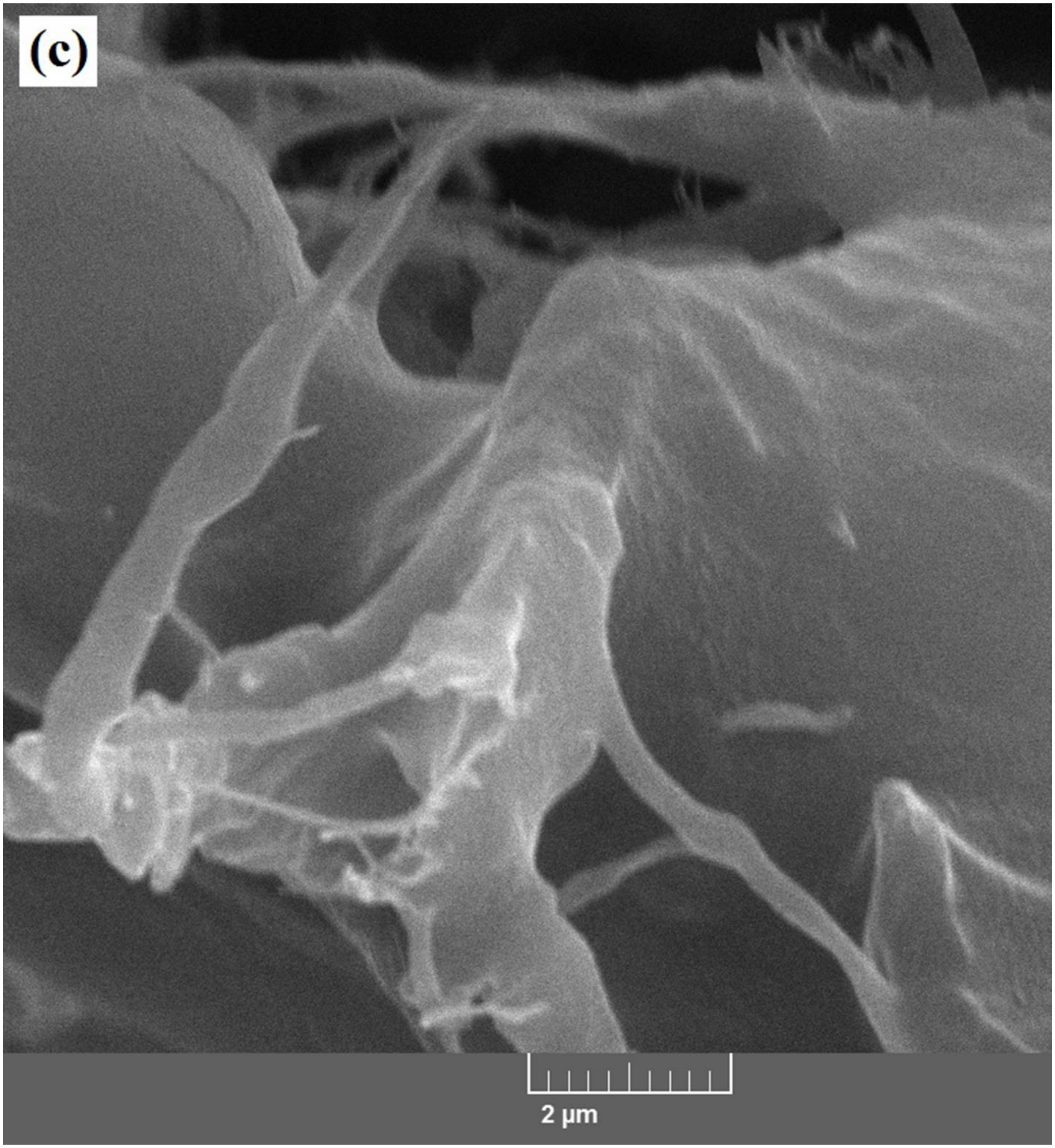

Figure 6 (c)

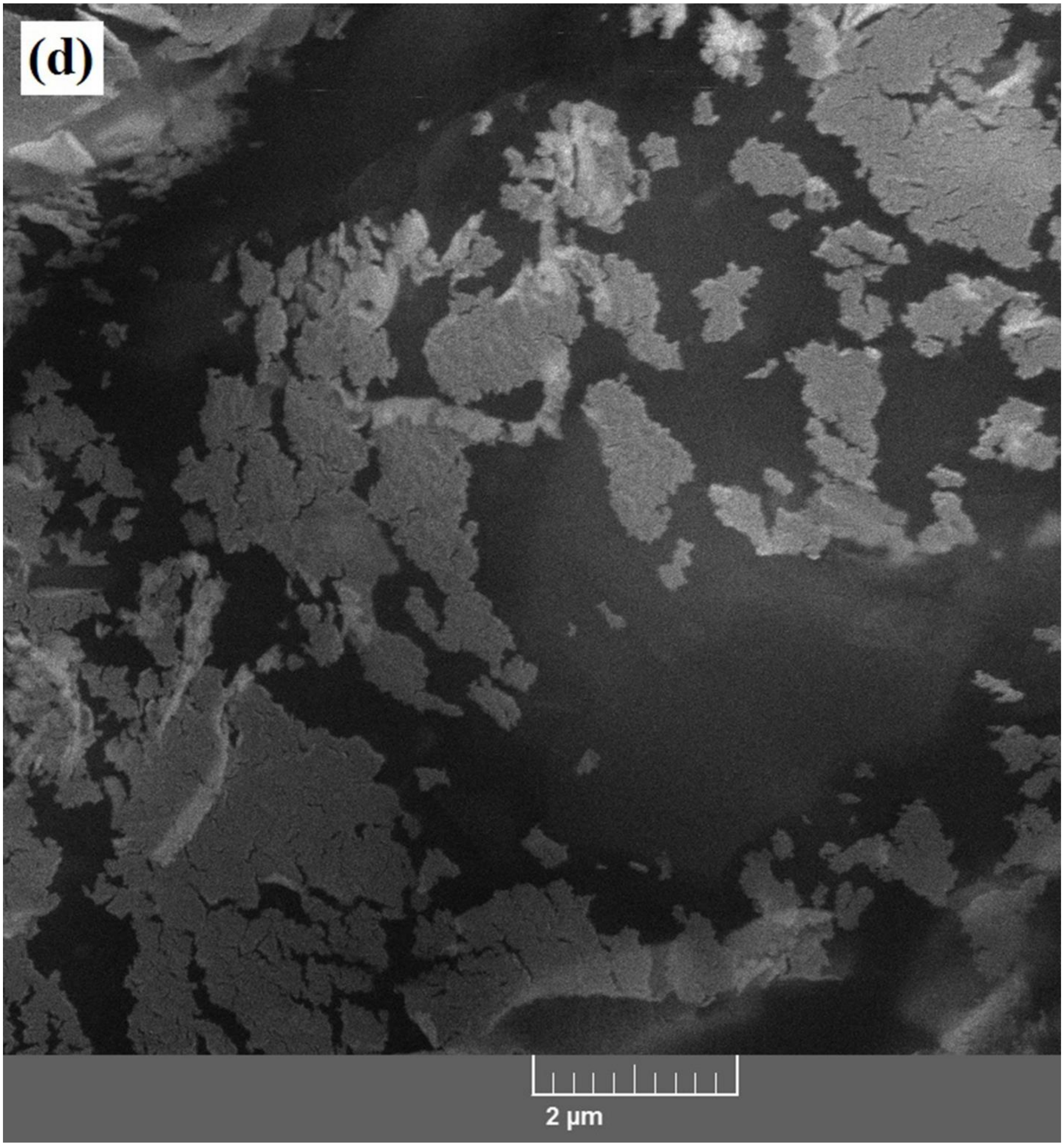

Figure 6 (d)

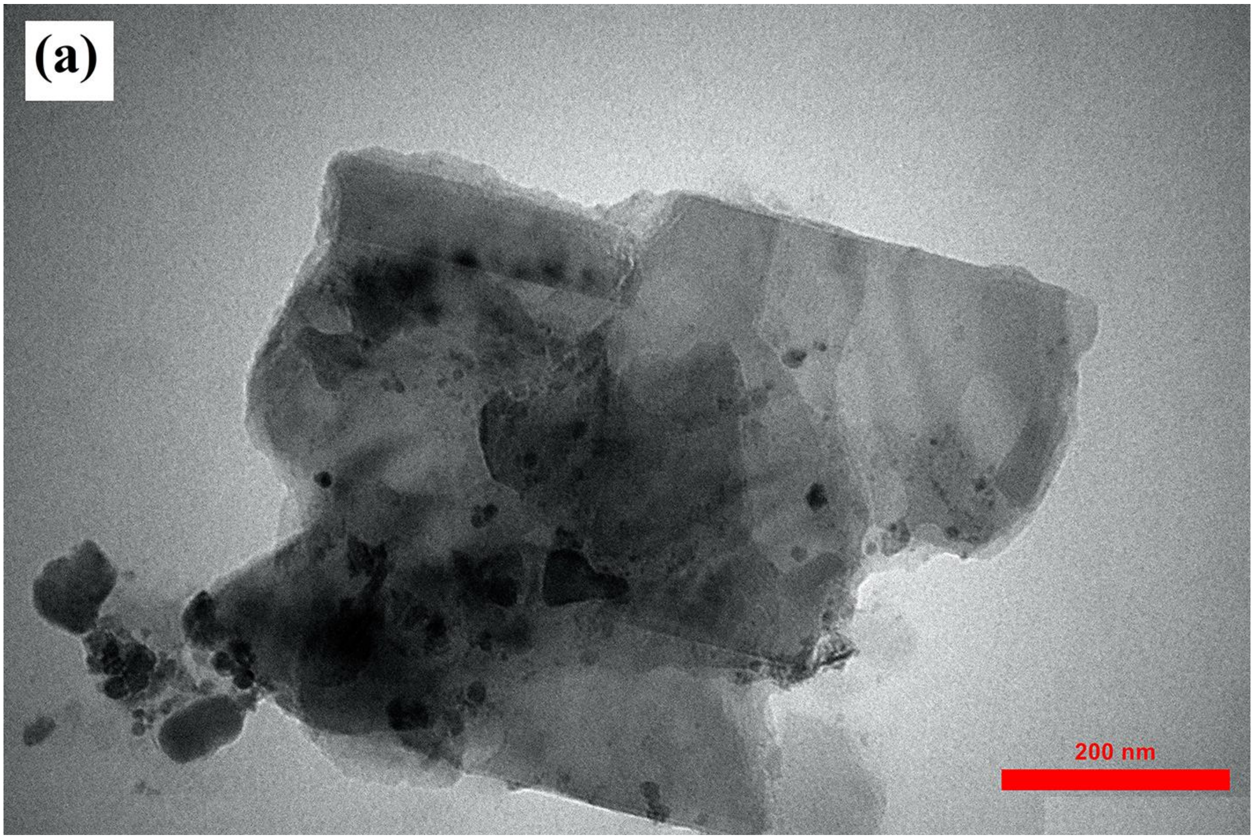

Figure 7 (a)

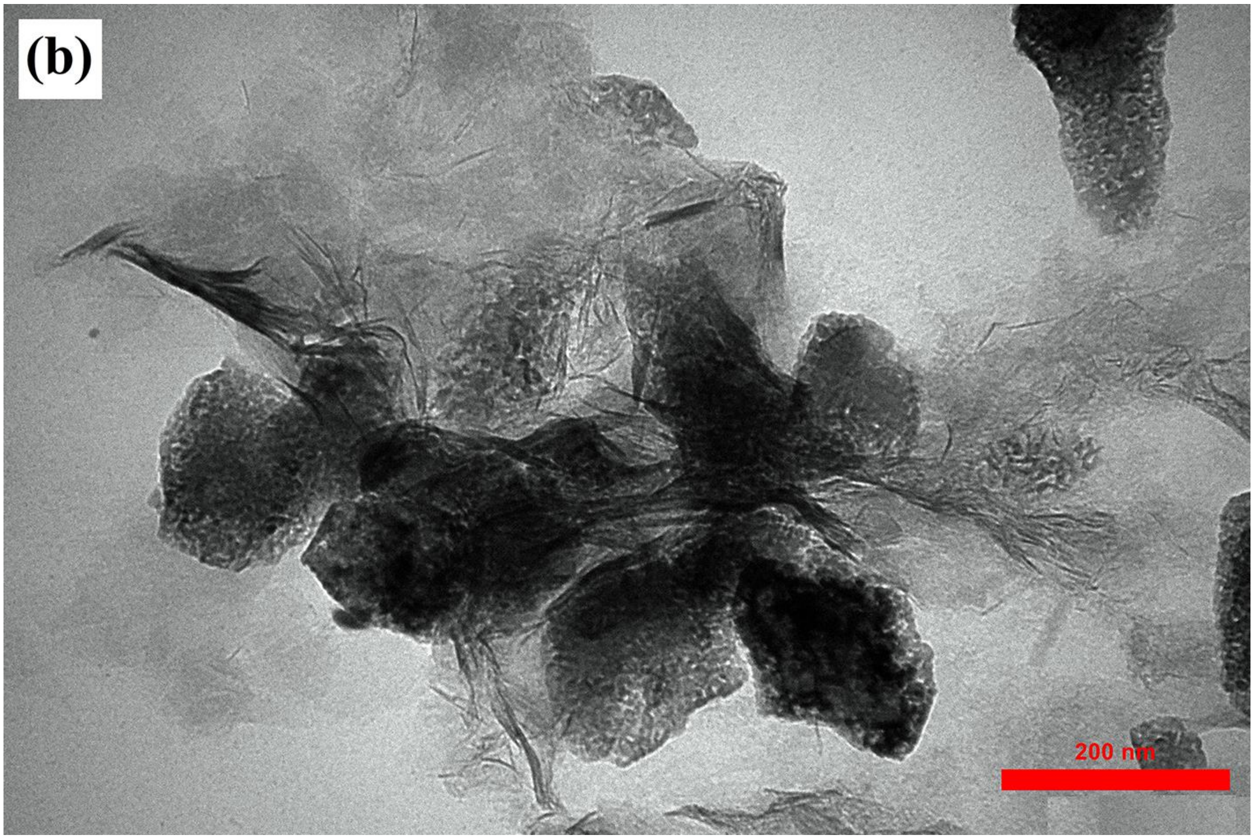

Figure 7 (b)

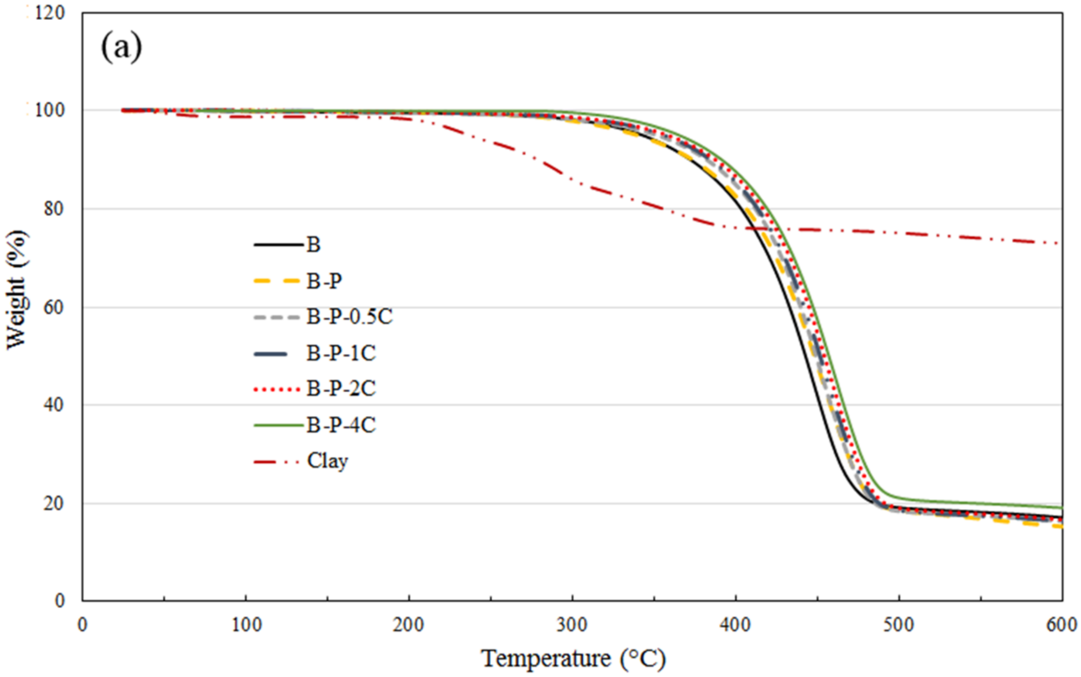

Figure 8 (a)

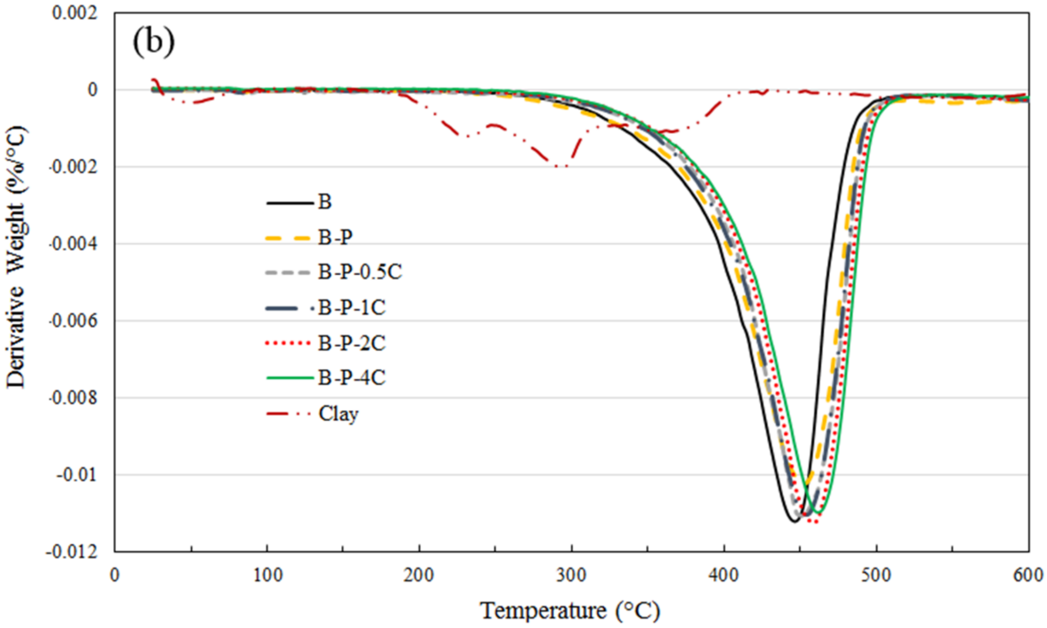

Figure 8 (b)

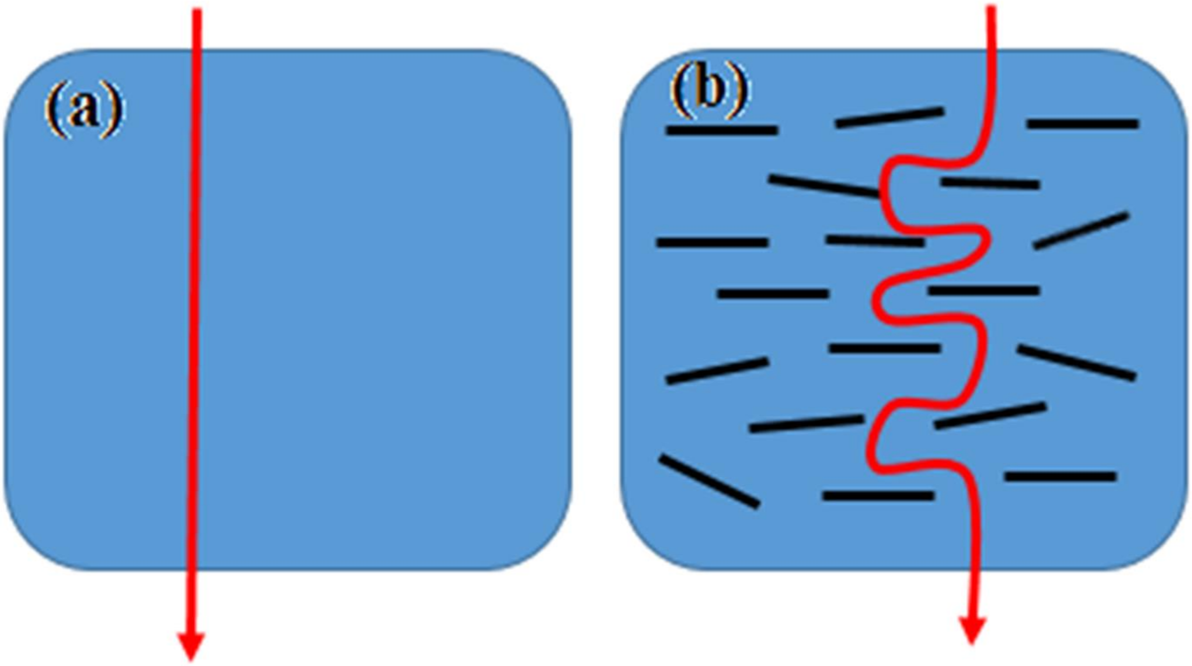

**Figure 9 a) and b)**

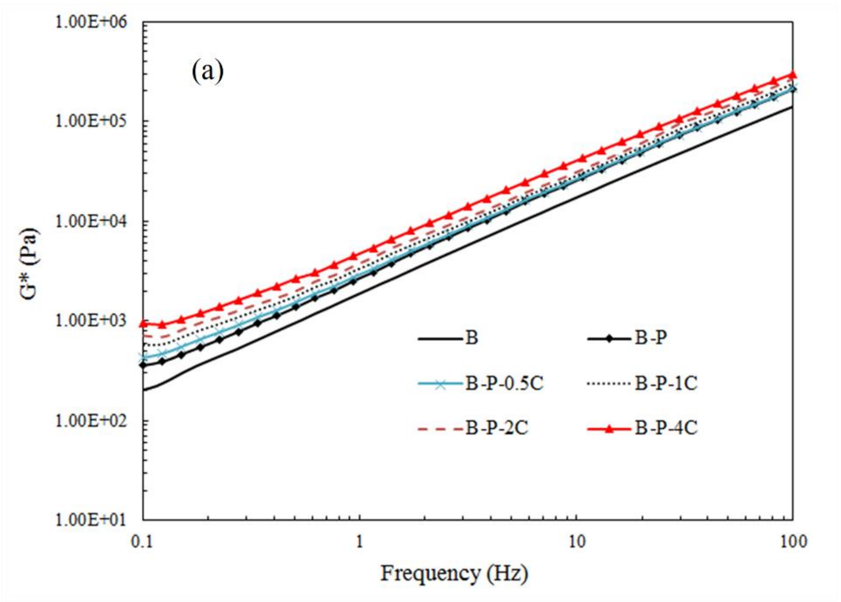

Figure 10. a)

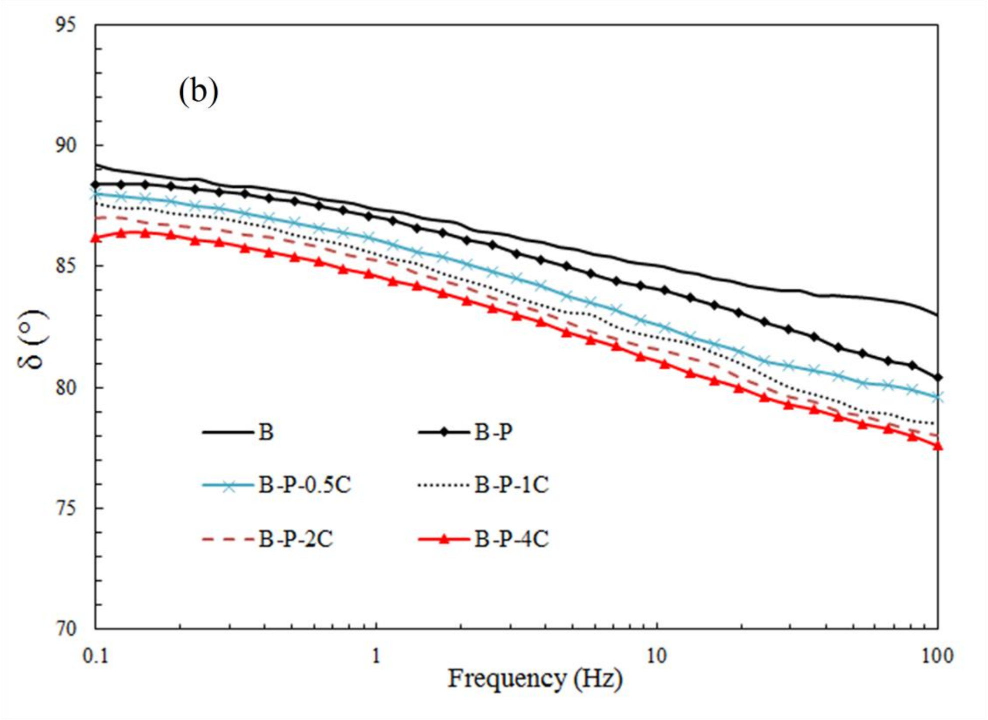

Figure 10. b)

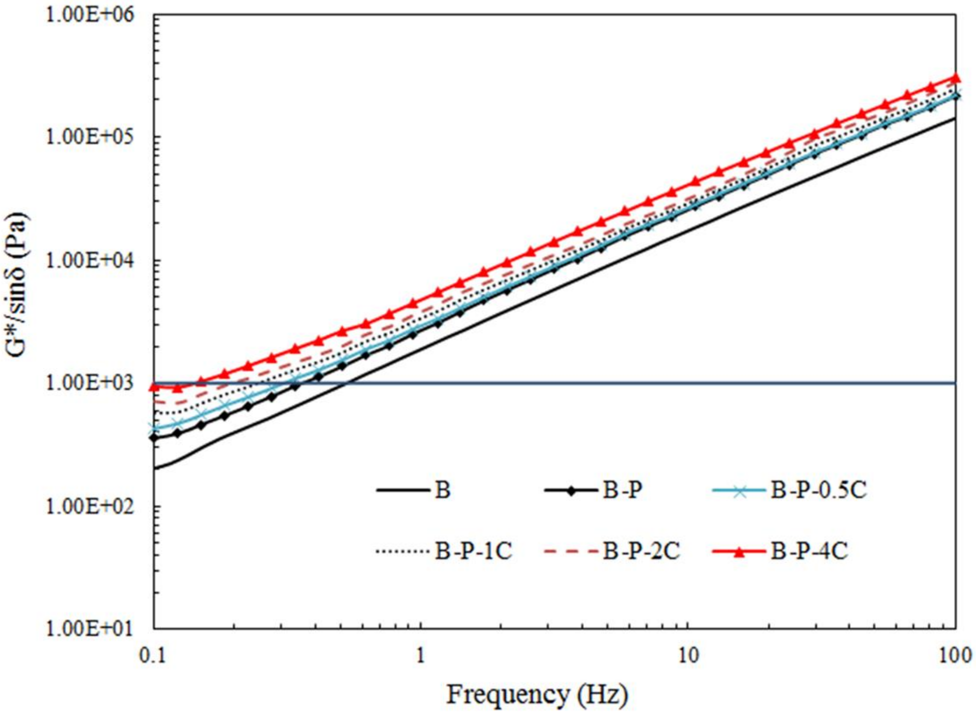
1.00E+06
1.00E+05
1.00E+04
1.00E+03
1.00E+02
1.00E+01
G*/sinδ (Pa)
0.1
1
10
100
Frequency (Hz)
B
B-P
B-P-0.5C
B-P-1C
B-P-2C
B-P-4C

**Figure 11**

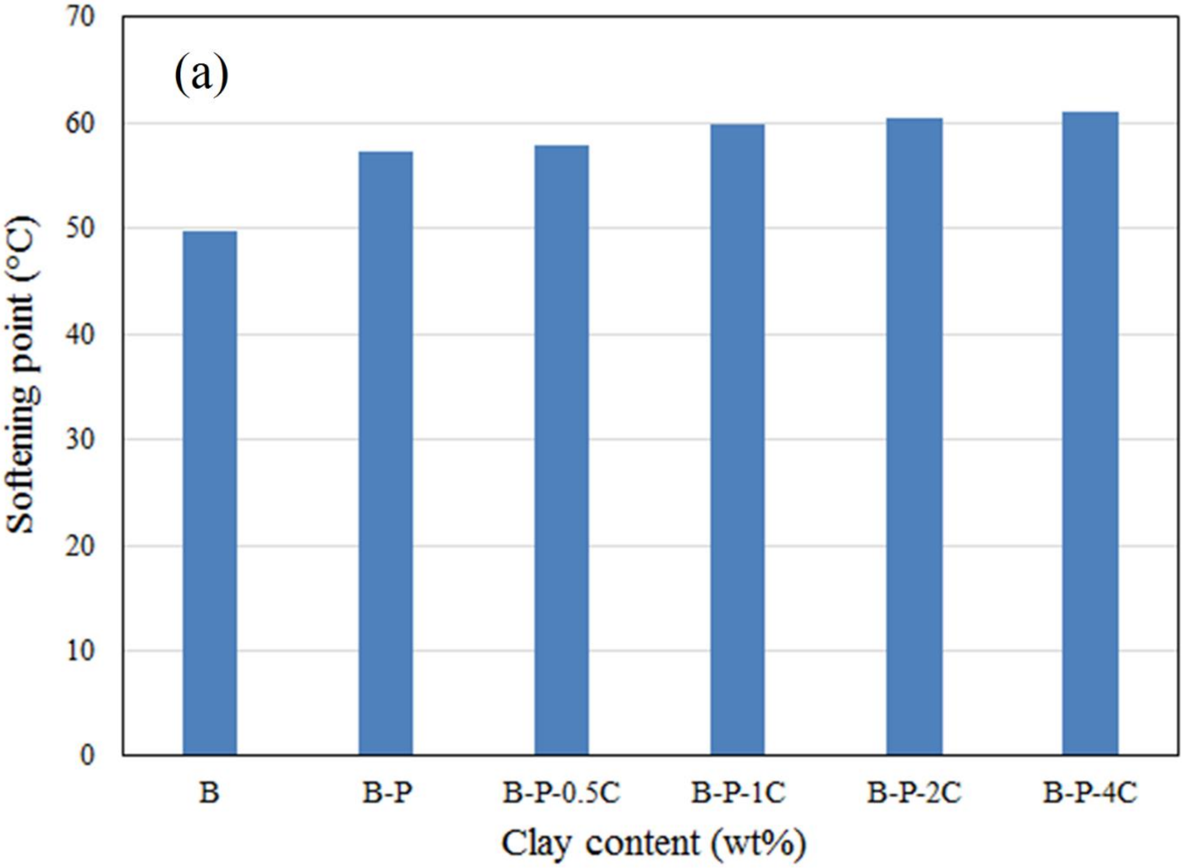
(a)
Softening point (°C)
70
60
50
40
30
20
10
0
B
B-P
B-P-0.5C
B-P-1C
B-P-2C
B-P-4C
Clay content (wt%)

**Figure12. a)**

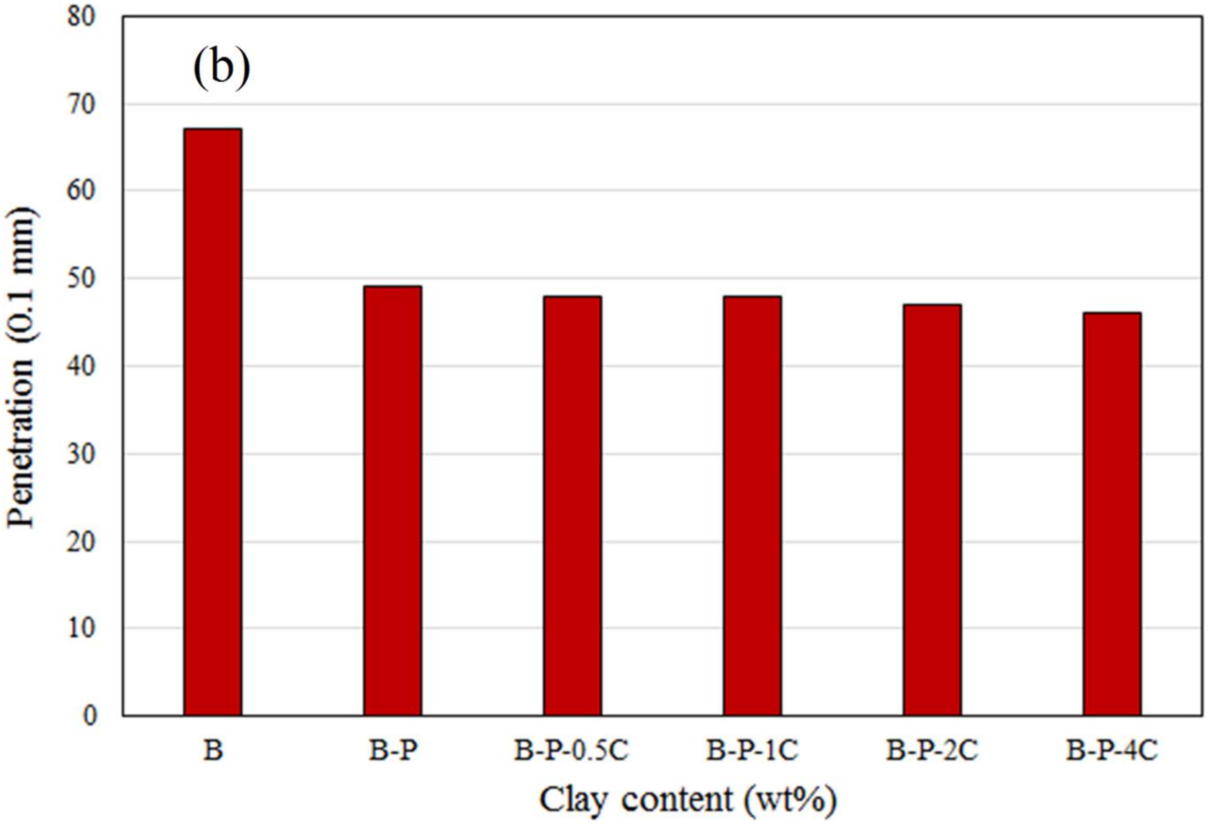
(b)
Penetration (0.1 mm)
0
10
20
30
40
50
60
70
80
B
B-P
B-P-0.5C
B-P-1C
B-P-2C
B-P-4C
Clay content (wt%)

**Figure12. b)**

## Tables:

TABLE 1

| Property | Unit | Limit |
|---|---|---|
| **Density@25˚C** | Kg/m3 | 1010-1060 |
| **Penetration@25˚C** | mm/10 | 60-70 |
| **Softening Point** | ˚C | 46 Min |
| **Ductility@25˚C** | cm | 100 Min |
| **Loss on heating** | Wt% | 0.2 Max |
| **Flash Point** | ˚C | 232 Min |
| **Viscosity@60˚C** | P | 2000±400 |
| **Viscosity@135˚C** | cSt | 300 Min |

TABLE 2

| Sample | Bitumen (g) | PET (g) | Clay (g) |
|---|---|---|---|
| **B** | 100 | - | - |
| **B-P** | 95 | 5 | - |
| **B-P-0.5C** | 94.5 | 5 | 0.5 |
| **B-P-1C** | 94 | 5 | 1 |
| **B-P-2C** | 93 | 5 | 2 |
| **B-P-4C** | 91 | 5 | 4 |

TABLE 3

| | B | B-P | B-P-0.5C | B-P-1C | B-P-2C | B-P-4C |
|---|---|---|---|---|---|---|
| **$T_{onset}$ (°C)** | 202.3 | 219.5 | 220.0 | 223.0 | 221.1 | 225.2 |
| **$T_{50\%}$ (°C)** | 442.7 | 447.8 | 449.1 | 451.4 | 454.1 | 457.1 |
| **$T_{max}$ (°C)** | 446.2 | 451.2 | 452.0 | 455.0 | 458.7 | 461.7 |

TABLE 4

| | B | B-P | B-P-0.5C | B-P-1C | B-P-2C | B-P-4C |
|---|---|---|---|---|---|---|
| **PI** | -0.55 | 0.40 | 0.48 | 0.88 | 0.95 | 1.02 |
| **Ductility (cm)** | >150 | 50.4 | 52.7 | 57.4 | 66.2 | 69.3 |

## Technical biography of authors:

**Fakhraddin Alimoradi** is a faculty of College of Engineering, Civil Engineering Group at Islamic Azad University, Chaloos Branch. He graduated in Civil Engineering from Sharif University of Technology, Iran in 1996. He obtained his MS in Civil Engineering (field of study: Hydraulic Structures) from Iran University of Science and Technology in 2001. He works in various fields of civil engineering including structure, construction, asphalt, bitumen and composites.

**Alireza Khaloo** is a distinguished professor in the Department of Civil Engineering at Sharif University of Technology, Tehran. His research interests include topics related to structural engineering, reinforced and prestressed concrete structures, composite materials, materials of construction, structural health monitoring, seismic strengthening, and earthquake engineering. Moreover, he has been involved in conducting different retrofitting projects such as refineries, petrochemical platforms, and sophisticated structures.

**Morteza Faghihi** is currently an Assistant Professor in Chemistry and Process Research Graoup at Niroo Research Institute (NRI) in Iran. He obtained his PhD in Chemical Engineering (field of study: Polymer Engineering) from Sharif University of Technology, Iran in 2015. His areas of Interests include Polymer, Composites, Nanocomposites, Adsorption and Water Treatment.